Kovove Mater. 61 2023 103–114
DOI: 10.31577/km.2023.2.103

Tribological performance of ceramic-based films under different tribo-test media and vacuum conditions

Yesim Zeynep Mandev, Ali Fatih Yetim*

Erzurum Technical University, Faculty of Engineering and Architecture, Department of Mechanical Engineering, Erzurum, Turkey

Received 20 July 2022, received in revised form 23 February 2023, accepted 6 March 2023

Abstract

The influence of different ceramic-based coatings on the adhesion and wear resistance of M2 high-speed steels has been investigated under different tribo-test conditions. For this purpose, TiN, CrN, and DLC films were deposited on the substrates and silicon wafers by a magnetron-sputtering PVD system. Structural, mechanical, and tribological properties of coated samples were examined with SEM, XRD, tribotester, microhardness and scratch tester. The sliding wear tests were performed under air, dry nitrogen, oil, and vacuum environments. It was seen that the highest hardness and residual stress values were obtained from the TiN-coated samples, while the lowest hardness and residual stress values were seen in the CrN-coated specimen. It was determined that the hardness and residual stress values of the coating were the most effective parameters between film and substrate adhesion. Therefore, it was observed that high hardness and residual stress had negative effects on critical load values. Tribological tests showed that the wear and friction behaviors differed from each other according to the coating type and tribo-test conditions. Both the lowest friction coefficient values and wear rates were obtained from the oil tribo-test environment. The lowest friction coefficient and wear rate values were achieved in DLC-coated samples.

K e y w o r d s: ceramic films, adhesion, wear, residual stress, vacuum

1. Introduction

High-speed steels, such as M2, are used for machining, die manufacturing and cutting tools operations, and they should withstand substantial mechanical and thermal stresses and chemical attacks. In addition, they are facing heavy wear-related problems in different service conditions. High-speed steels are frequently subjected to high contact pressures under sliding wear conditions [1]. Therefore, it is very important to prolong their service life and cutting performance due to the commercial value of these products. Surface texture is one of the important methods to improve the tribological properties of materials. Surface texture can be produced by laser or formed in situ [2–5]. Surface modification and/or coating methods, plasma diffusion processes, PVD and CVD coatings, and ion/electron beam treatments are commonly applied to tool steels to increase tool life.

Ceramic-based hard coatings are a very suitable candidate to increase the durability of the tool materials used in severe wear and aggressive environments [6, 7]. In this respect, coating materials such as CrN, TiN, TiC, TiAlN, NbN, MoS_2, DLC, and their multi-layer combinations have been successfully used in many industrial applications [8–14]. Among these coating materials, CrN and TiN coating materials have been popular for many industrial applications for a few decades due to their relatively low friction coefficient, high hardness, toughness, and corrosion resistance [9, 15–17]. Wilson et al. [18] have noted that the wear resistance of CrN is better than that of TiN. In addition, it has been stated that CrN can be deposited more thickly than TiN [6, 19]. Some researchers thought that the thickness of the coating affected the residual stresses and stress distribution under contact conditions, and these stresses may cause adhesion problems and then coating failure [20,

*Corresponding author: tel.: +90 444 5388-2063; e-mail address: fatih.yetim@erzurum.edu.tr

Table 1. Chemical compositions of M2 high-speed steel substrates (wt.%)

Fe	Cr	V	W	Mn	Si	Mo	C
Balance	4.1	1.7	6.4	0.3	0.5	5.3	0.9

21]. Also, deposition technique and parameters, microstructure and morphology are very important in coating performance in service conditions. S. H. Yao et al. [22] studied the tribological behavior of CrN, Cr(C,N), and TiN-coated steel samples with using a reciprocated sliding wear test machine. In this study, it was observed that CrN coating showed higher wear resistance compared with TiN. Mansoor et al. [23] investigated the tribological properties of TiN/CrN, CrN, and TiN coatings, and it was seen that all coatings reduced the coefficient of friction and wear rate. Y. L. Su et al. [24] compared the tribological properties of TiN, TiCN, and CrN under dry and lubricated conditions. Results showed that CrN was a good candidate for engineering applications demanding wear resistance. Diamond-like-carbon (DLC) films have great potential to be used as protective coatings to enhance the tribological behavior of materials because DLC films have relatively higher hardness, chemical inertness, good wear resistance, and low friction coefficient [11, 25–29]. However, DLC films have some problems, such as relatively high intrinsic film stresses. These problems can cause low adhesion and the deterioration of DLC films [10, 30]. The increasing demands for improved coating life lead to the deposition of multilayer and/or duplex coatings. The constitution of such graded structures provides a high load-carrying capacity. Hence, the tribological performance of ceramic-based films is improved [1, 29, 31, 32].

The main aim of this study is to compare the relationship among wear, residual stresses, and adhesion of the films under air, dry nitrogen, oil, and vacuum tribo-conditions. For this purpose, TiN, CrN, and DLC coatings commonly preferred in tool steels were deposited by the magnetron sputtering PVD method. Detailed structural, mechanical, and tribological characterization of these coating materials was investigated by means of SEM, XRD, tribo and scratch tester.

2. Experimental details

In this study, TiN, CrN, and DLC films were deposited on AISI M2 high-speed tool steel substrates and silicon wafers. The chemical composition of the substrates is given in Table 1. The substrates were ground by 220–1200 mesh emery-papers, and then polished with alumina powders with 0.1 μm grain size. After cleaning with distilled water and alcohol, AISI M2 samples and silicon wafers were used for analyzing the film thickness and structural properties of coatings. For these processes, samples were placed in a magnetron sputtering PVD system (VAKSIS PVD-MT/2M 2T), and the system was evacuated to 2×10^{-3} Pa. Before TiN, CrN, and DLC deposition, samples were subjected to ion sputtering with Ar gas for 30 min to remove possible contaminants. Then, the Ti interlayer was deposited at 6 A current for 250 V bias and for 0.4 Pa pressure for 5 min to improve adhesion between the film and the substrate for all coatings. TiN, CrN, and DLC films were deposited on the samples by the coating parameters given in Table 2.

After coating processes, phase and residual stress analyses were determined by GNR-Explorer XRD device with Cu-Kα radiation source operated at 30 kV and 30 mA with wavelength $\lambda = 1.5405$ Å. The obtained phase compositions were compared with the PDF-4 peak lists. The residual stress measurements were performed with an incident angle of 1° using the $\sin^2\psi$ method. Shimadzu HMV-G20 microhardness tester was utilized for microhardness values. The microhardness measurements were performed with the Knoop method at a constant load of 10 g and a dwell time of 15 s. Bruker-UMT (Bruker Universal Mechanical Tester) tribometer tester was used for scratch test to determine the adhesion of the coatings. Standard adhesion tests were performed with a 120° conical Rockwell-C diamond indenter to measure critical loads.

The friction and wear properties of the films were examined in the air with a relative humidity of ∼ 50 %, in dry nitrogen at room temperature, in boron oil coolant and under vacuum condition of 10^{-6} mbar. A pin-on-disk tribo-tester (Bruker Universal Mechanical Tester-UMT) was used to determine the tribo-

Table 2. Mechanical, adhesion, and tribological test results

Sample	Surface hardness $HV_{0.01}$	Surface roughness, R_a (μm)	Layer thickness (μm)	Residual stress (GPa)	Elastic modulus (GPa)	Critical load, L_{c1} (N)
M2 substrate	300–320	0.01	–	–	210	–
TiN	1150–1200	0.026	1.5–2	–6.47	600	25
CrN	1250–1300	0.022	1.5–2	–2.10	200	50
DLC	1000–1050	0.025	1.5–2	–3.25	120	47

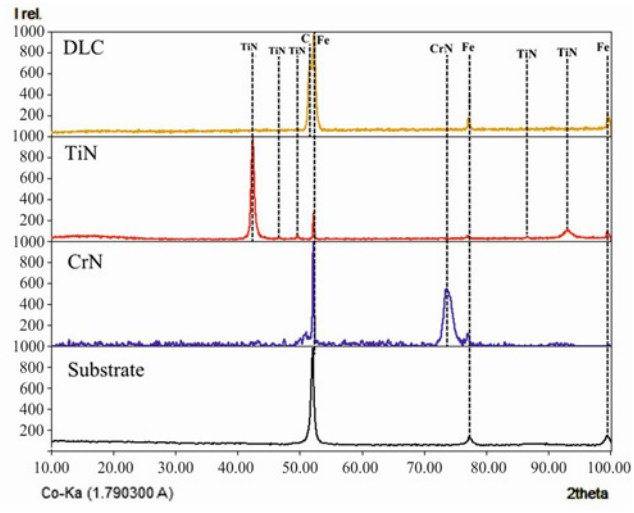

Fig. 1. XRD patterns of TiN, CrN, and DLC coated samples.

logical properties of the films. All experiments were conducted with 6 mm diameter alumina (Al_2O_3) balls in sliding contact and carried out with a load of 5 N and a total sliding distance of 141 m. A 3D optical microscope (Bruker Contour GT-I 3D, USA) was used to determine wear volumes and 3D surface profiles of samples. The thickness, microstructure, and morphology of the films and worn surfaces were investigated by an ESEM (FEI QUANTA-FEG 450, USA).

3. Results and discussion

3.1. Structural and mechanical analysis

The XRD patterns of untreated, TiN, CrN, and DLC-coated M2 high-speed steel samples are shown in Fig. 1. The typical α-Fe phase diffractions are clearly seen for untreated samples. According to coating type, characteristic TiN, CrN, and C/TiC peaks were observed together with α-Fe from the substrate due to relatively thin coating thicknesses. XRD technique ($\sin^2\psi$ method) was also used to determine the residual stress values of coatings. The $\sin^2\psi$ technique is identical to the two-angle technique, except lattice spacing is determined for multiple ψ tilts, a straight line is fitted by least squares regression, and the stress is calculated from the slope of the best fit [33]. The obtained values are given in Table 2. The compressive residual stresses were obtained from all coated samples. The highest residual stress values were measured for the TiN-coated samples.

The cross-section SEM images of TiN, CrN, and DLC films deposited on silicon wafers are given in Fig. 2. Silicon wafers were used to easily determine film thicknesses and microstructures. Titanium interlayer deposited onto substrates to improve adhesion between the film and the substrate is obvious from Fig. 2. On the titanium interlayer, homogeneous, dense, and compact structures were observed from all coatings. It was seen that the CrN film was denser and had a thinner columnar structure than both TiN and DLC films. Additionally, any crack, gap or struc-

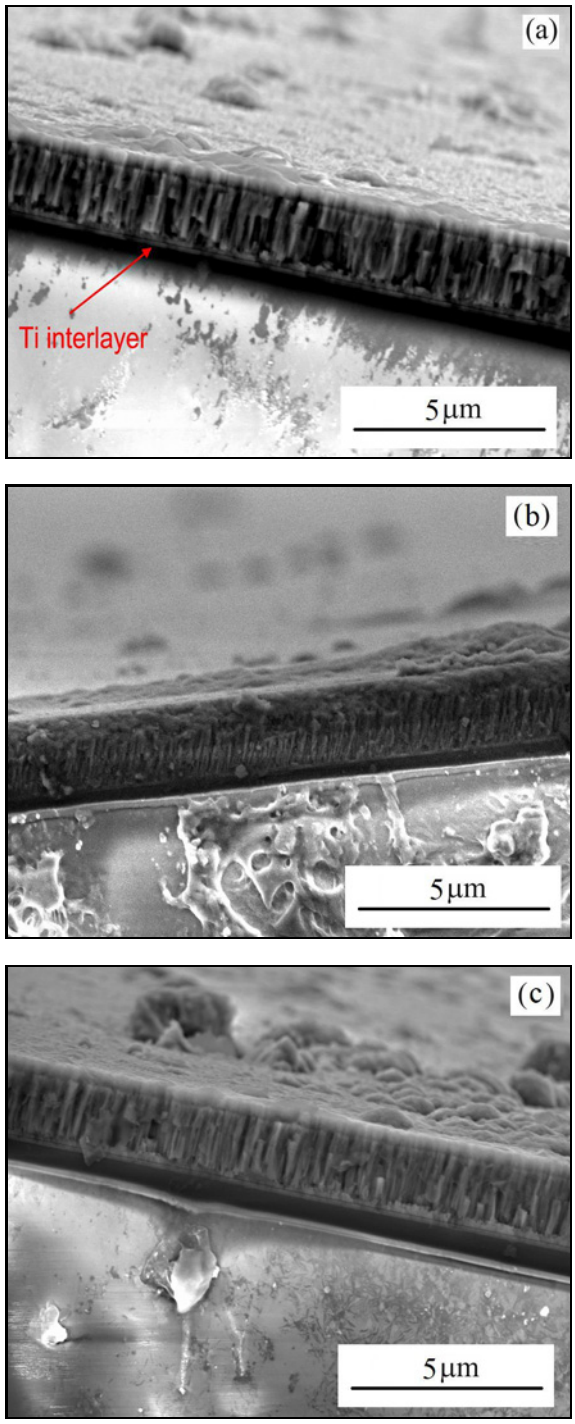

Fig. 2. Cross-section SEM images of deposited films on silicon wafers: (a) TiN, (b) CrN, and (c) DLC.

tural defect was not seen in the films. The columnar structure of the films increased the surface roughness of coated samples. While the mean surface roughness (R_a) of the untreated M2 samples was 0.01, this value increased up to 0.022, 0.025, and 0.026 µm for CrN, DLC, and TiN films, respectively. The thicknesses of the coatings were measured from the silicon wafer samples because silicon wafer samples were broken, and the integrity of the films was maintained. The films of equal thicknesses of about 2 µm were grown for accurate evaluation and comparison of tribological and adhesion properties.

Microhardness values of untreated and coated samples are given in Table 2. While the microhardness of untreated M2 steel was measured at about 300 $HV_{0.01}$, surface hardness values increased up to 3–4 times depending on the coating type. Ceramic-based films increased the load-carrying capacity of the surfaces and reduced the plastic deformation that may possibly occur against the load applied by the indenter. The highest hardness values were measured for CrN-coated samples due to denser and more compact structure.

Graphs of scratch test results for TiN, CrN, and DLC thin film coatings are given in Fig. 3. Scratch tests have been used to determine the adhesion of the thin coatings. Bull [34] recommended the most common version for scratch tests. According to this ver-

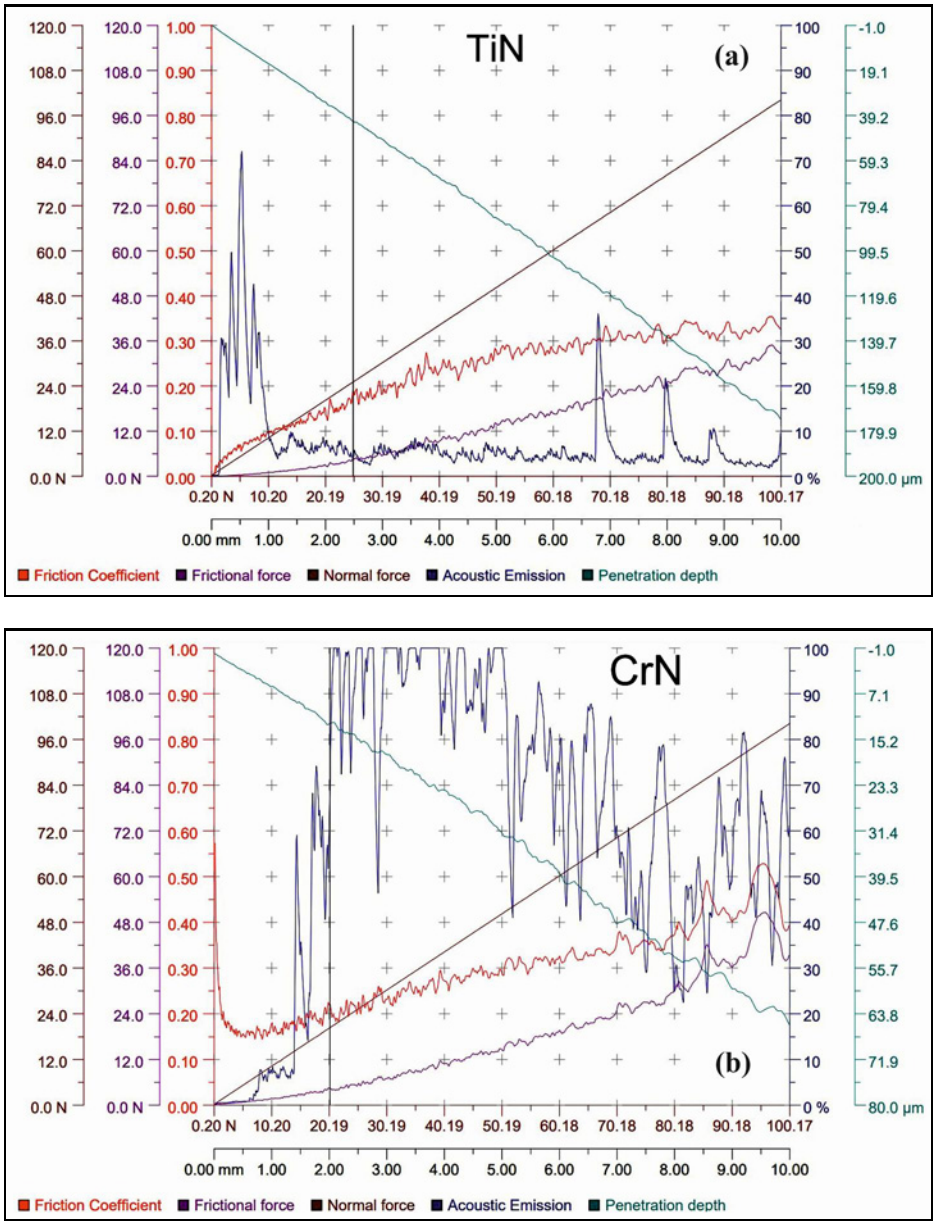

Fig. 3a,b. Scratch test results: (a) TiN, (b) CrN.

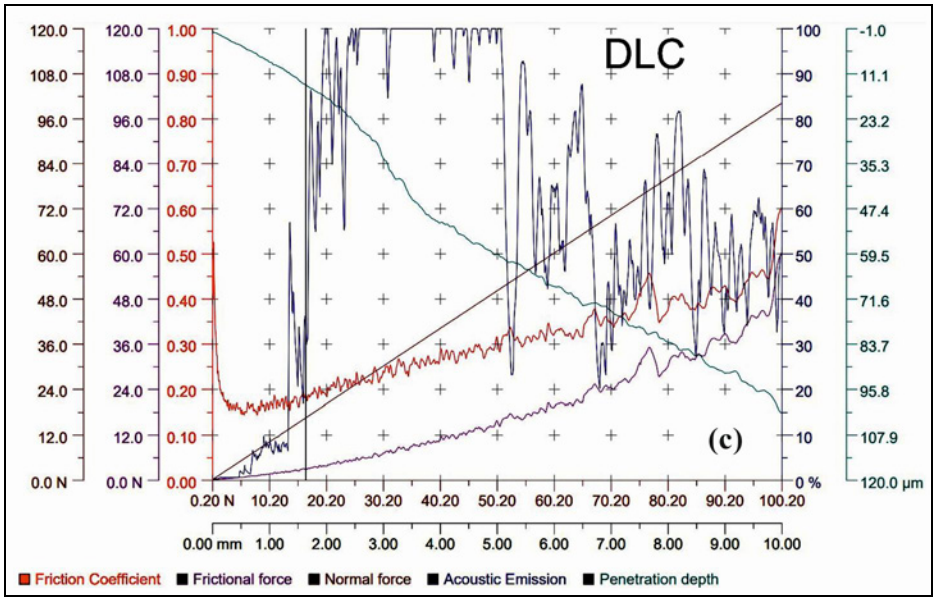

Fig. 3c. Scratch test results: (c) DLC.

Table 3. Tribological test results under different test conditions

Sample	Wear rates ($mm^3\ N^{-1}m^{-1}$)				Average friction coefficients			
	Air	Dry nitrogen	Oil	Vacuum	Air	Dry nitrogen	Oil	Vacuum
M2 substrate	1.91×10^{-4}	2.41×10^{-4}	7.69×10^{-5}	2.91×10^{-4}	0.71	0.78	0.30	0.91
CrN	2.51×10^{-5}	2.98×10^{-5}	5.76×10^{-6}	8.41×10^{-5}	0.39	0.46	0.18	0.55
TiN	3.24×10^{-5}	3.81×10^{-5}	7.91×10^{-6}	5.66×10^{-5}	0.30	0.35	0.16	0.44
DLC	1.23×10^{-5}	1.45×10^{-5}	2.13×10^{-6}	2.95×10^{-5}	0.20	0.24	0.09	0.28

sion, an indenter is drawn across the coated surface under a progressive loading until a defined failure occurs at a load which is called the critical load L_C. The critical load can be determined using both acoustic emission and optical methods. The scratch tests results showed that the first critical load values (L_{C1}) of TiN, CrN, and DLC thin films deposited on M2 high-speed steel substrates were measured as 25, 50, and 47 N, respectively. As well known, the thickness, hardness, and internal stresses in the film significantly affect the adhesion of the film to the substrate. Among the coatings examined in this study, all films of equal thickness were deposited to eliminate the effect of film thickness. It was observed that although the TiN film had the highest hardness, it exhibited the lowest critical load value. In this case, it was determined that the most effective parameter that affects the film adhesion was the internal stress in the film. Optical scratch track images of coatings are shown in Fig. 4. It was seen that a cohesive failure mechanism occurred in all the films. A compressive and buckling spallation ahead of the indenter was typically observed both inside and on the edge of the scratch track for TiN films. This failure type occurs in response to the compressive stresses generated ahead of moving indenter [34]. On the other hand, conformal cracking and flaking were seen for CrN and DLC films (Figs. 4b,c). As the applied load increased, flaking occurred along the edge and inside the tracks.

3.2. Tribological examinations

The variation of friction coefficient versus time and average friction coefficient values of untreated, TiN, CrN, and DLC-coated M2 high-speed steel are given in Fig. 5 and Table 3. When Fig. 5 is examined, it can clearly be seen that the behavior of the friction coefficient of all samples with time was similar from the beginning to the end of the tribological tests. It was observed that the friction coefficients reached to a maximum at the initial stage of the friction tests due to Hertzian contact, then became a steady-state behavior with matching and smoothing of the sliding surfaces. Friction coefficient graphs showed a run-in-period behavior for both untreated and coated samples at the beginning of sliding [11]. It was calculated that the mean friction coefficient values in the steady state changed with a standard deviation of 0.01. On the

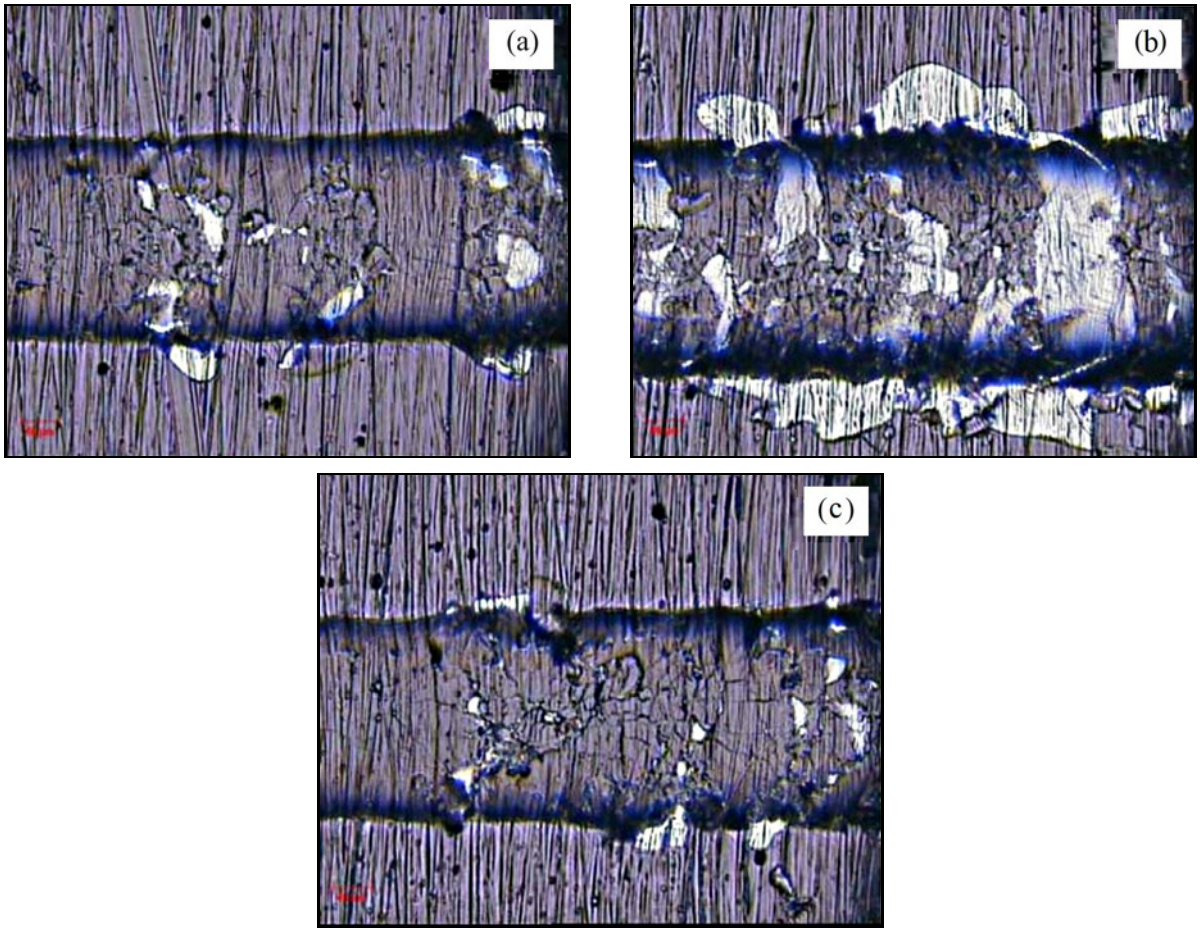

Fig. 4. Optical images of scratch tracks: (a) TiN, (b) CrN, and (c) DLC.

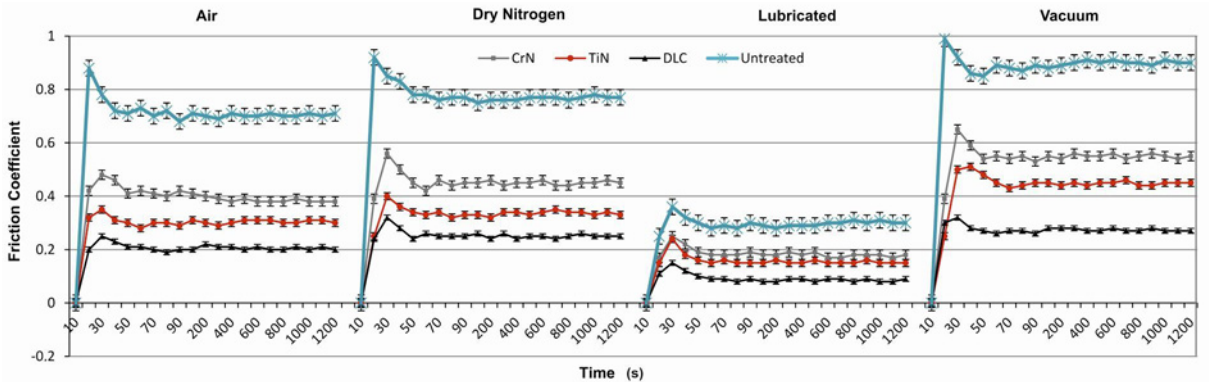

Fig. 5. Friction coefficient vs. time graphs of untreated, TiN, CrN, and DLC-coated samples tested under different tribological environments.

other hand, average friction coefficient values changed under different sliding environments. While the highest friction coefficient values were obtained from samples worn under vacuum, the lowest friction coefficient values were seen in the samples tested under a lubricated environment as expected. It was determined that the friction coefficient values increased due to a lack of oxidation of the surfaces of the untreated samples under vacuum conditions. Although all three types of coatings reduced the penetration depth of the pin and caused sliding at low shear stresses, the self-lubricating property of the graphitic structure in DLC structure caused the lowest friction coefficient values to be obtained from DLC samples even in high vacuum conditions. A transfer film is thought to form between the pin and the coating due to the relatively

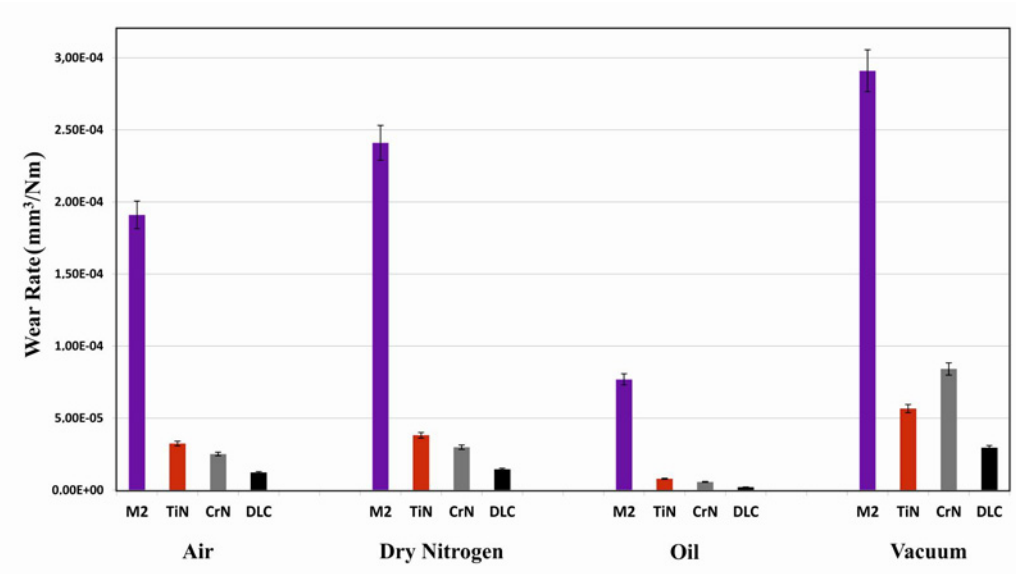

Fig. 6. Comparison of wear rate values of untreated, TiN, CrN, and DLC-coated samples tested under different tribological environments.

low cohesion resistance of DLC films. It was believed that the lowest coefficient of friction values was to be seen in DLC-coated specimens in different wear environments because the Al_2O_3-DLC contact changed to DLC/DLC contact during sliding.

The wear rates of untreated, TiN, CrN, and DLC-coated samples worn under different sliding conditions are shown in Fig. 6 and Table 3. It was seen that the wear resistance of the M2 surface increased after applying surface treatments, as expected. It was thought that film thickness, hardness, surface roughness, stresses in the film and adhesion between the film and the substrate have important effects on the wear behavior of the surface. An enough thick and hard coating increased the load-bearing capacity of the substrate/film tribo-system and increased the wear resistance of the surface compared to the untreated samples. In addition, the type of mating bodies as well as these factors, will affect the wear resistance. The transformation of metal/ceramic contact to ceramic/ceramic contact will also affect wear resistance. In this study, since the films were deposited to have approximately equal film hardness, thickness, and roughness, it was seen that the most important parameters of wear resistance were hardness, residual stress, chemical composition, and adhesion of the films. According to this point of view, the lowest wear rates were expected in CrN-coated samples, while the lowest wear rates were obtained in DLC-coated samples due to the increased load-bearing capacity of the film and the solid lubricating property of the diamond/graphite structure. The lattice structure of DLC tends to slide between the basal planes with low shear stresses. For this reason, DLC film coating emerges as a solution in situations where there is a lack of oxidation, and it is not possible to lubricate with chemical lubricants, such as in vacuum conditions. Considering all wear environments tested this in the study, the lowest wear rates were obtained for both untreated and coated samples in the wear tests performed in oil media, since it formed a film that facilitated sliding between the contacting surfaces.

Characteristic SEM images of wear paths and three-dimensional (3D) typically worn surface images of untreated and all coated samples worn under humid air, dry nitrogen, oil and vacuum conditions are shown in Figs. 7 and 8, respectively. The worn surface of the untreated sample showed that M2 high-speed steel was exposed to high plastic deformation, adhesive and micro-abrasive wear. Pile-ups on the wear track edges are indicative of extensive shear deformation and, thus, plastic deformation during wear. In addition, obviously seen plate-like wear debris indicated adhesive wear (Fig. 7a). These kinds of debris occur when the cold weld-like bonds formed during metal/ceramic pin contact are broken by relative sliding movement, and the relatively soft ruptured part is smashed between the pin and the substrate by the effect of the applied load. In addition, the ground hard micro-debris led to the micro-abrasive marks in the wear track (Fig. 7a). In the case of coated samples, it is generally seen that the wear behavior of the coated samples changed, and excessive plastic deformation and adhesive wear were prevented by the hard and high load-carrying capacity films deposited on the surfaces. On the other hand, it was observed that the wear marks of the TiN and CrN-coated samples exhibited generally similar properties. Although the hardness values of TiN-coated samples were relatively higher than those of CrN-coated ones, the higher

residual stresses in the TiN films and the weak adhesion caused brittle debris to form more easily during sliding, resulting in higher wear rates according to CrN samples (Figs. 7b,c). DLC-coated samples showed a different behavior compared to TiN and CrN-coated samples. While the diamond structure within the DLC provided the load-carrying ability of the film, the graphitic structure showed solid lubricant behavior. In this way, a transfer film was formed between the pin and the DLC structure, and the Al_2O_3 pin/DLC contact changed to DLC/DLC contact during the wear test. The smashing, flaking, and delamination of the transfer film that breaks over time during sliding can be seen in Fig. 7d. The wear behavior of untreated and coated specimens was generally found to be similar for different wear environments. It is thought that

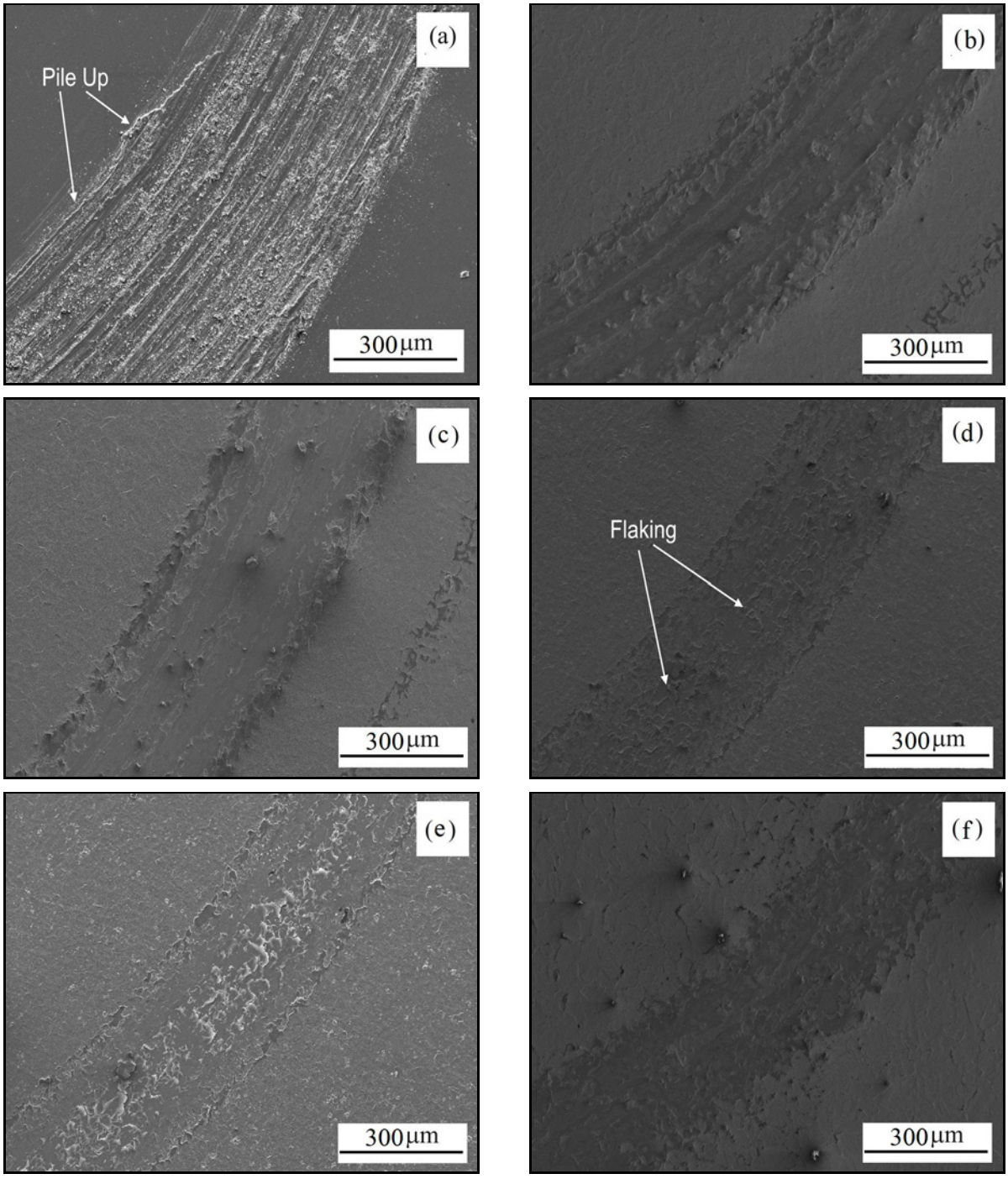

Fig. 7a–f. Typical SEM images of wear tracks: (a) Untreated/Humid Air, (b) TiN/Air, (c) CrN/Air, (d) DLC/Air, (e) DLC/Dry nitrogen, (f) DLC/Oil.

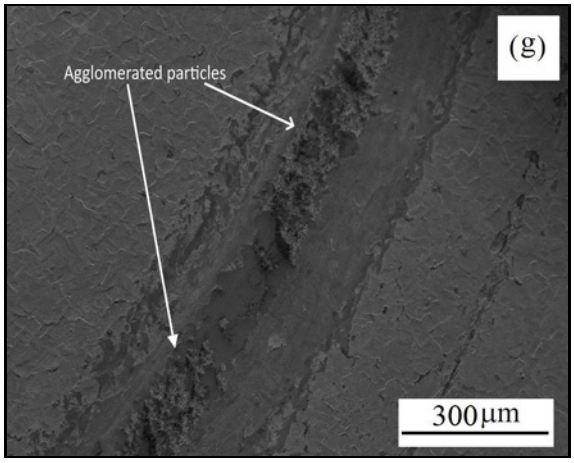

Fig. 7g. Typical SEM images of wear tracks: (g) DLC/Vacuum.

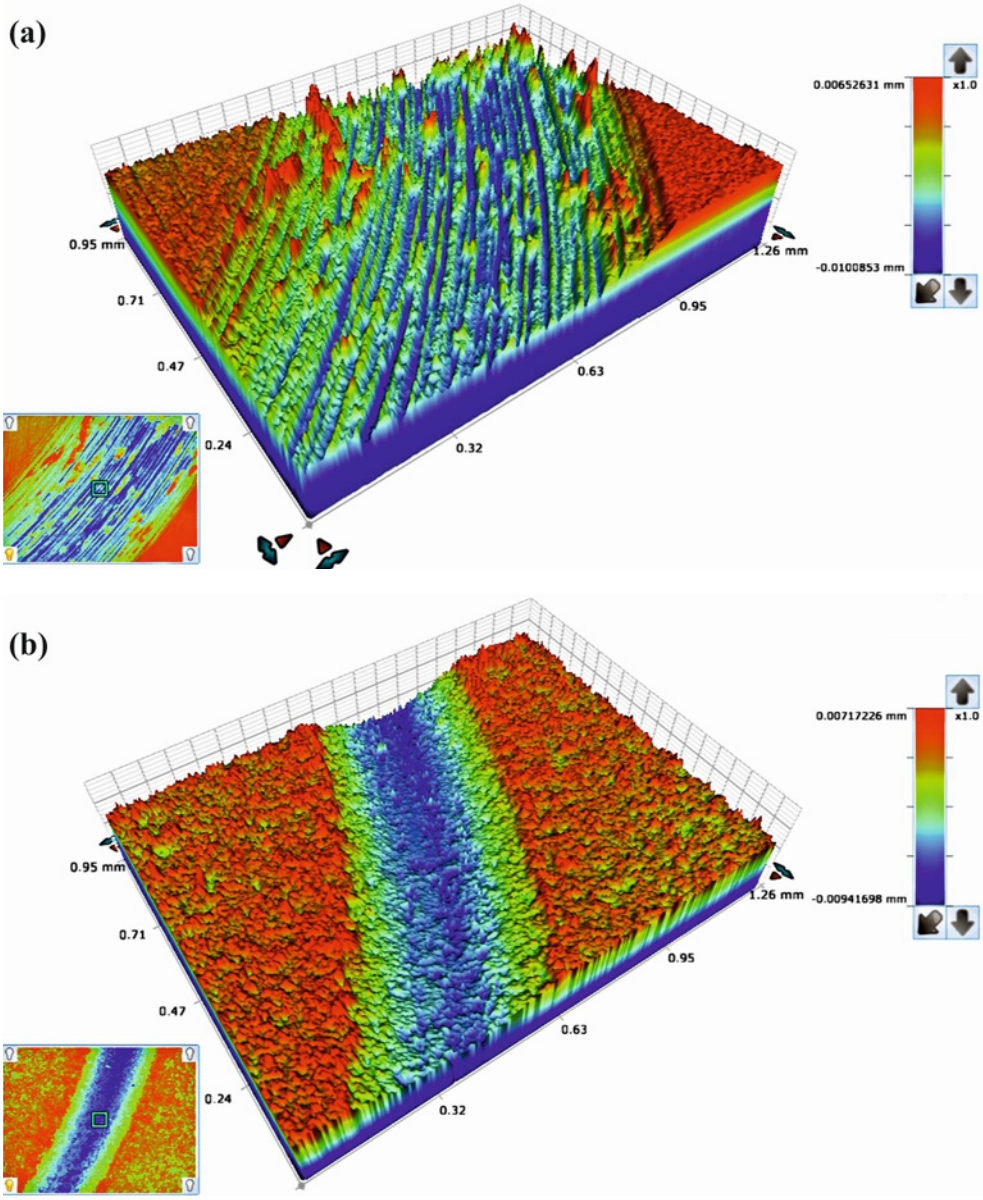

Fig. 8a,b. Typical 3D optical worn surface images of the samples: (a) Untreated, (b) TiN.

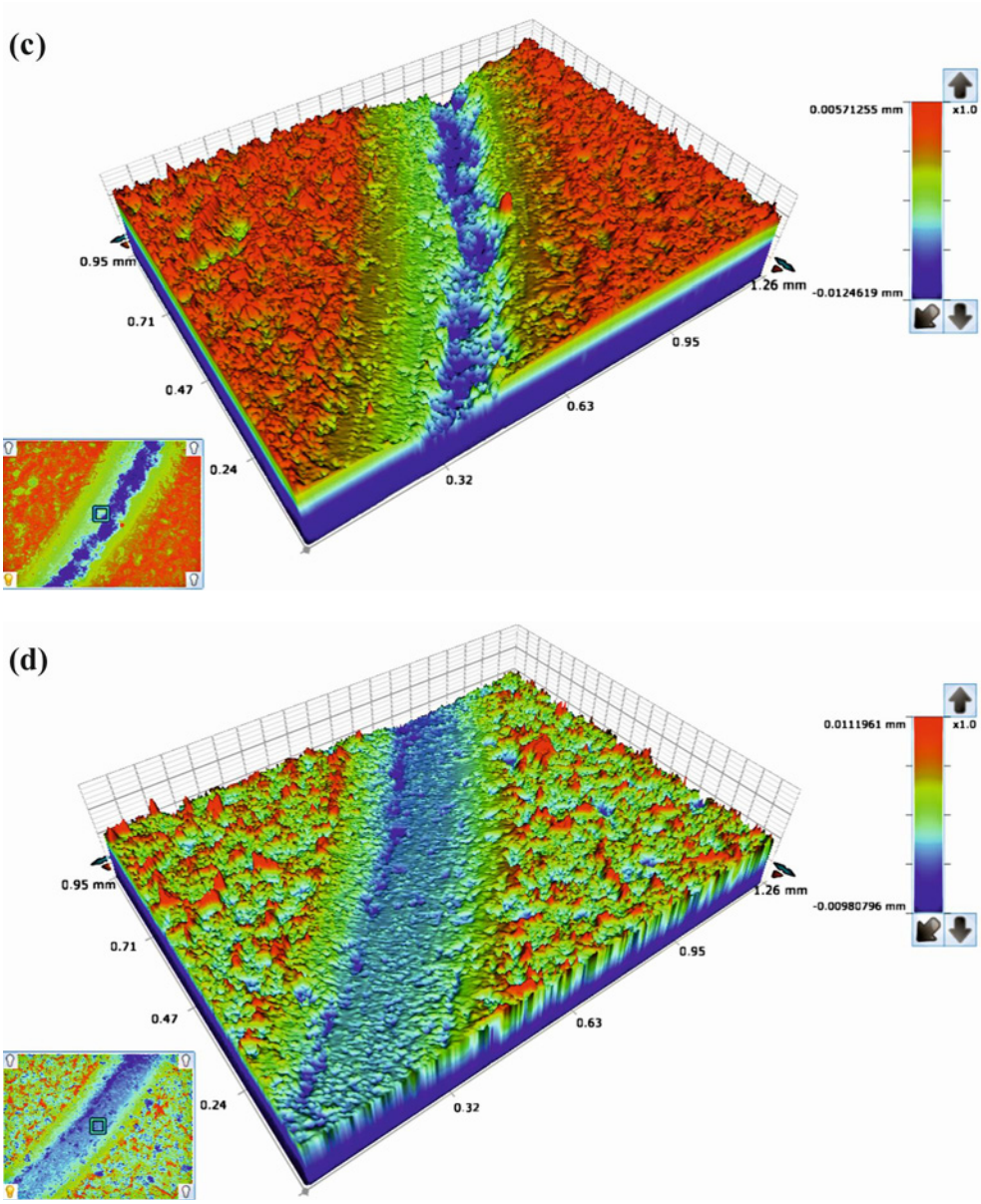

Fig. 8c,d. Typical 3D optical worn surface images of the samples: (c) CrN, and (d) DLC.

the hard and brittle wear debris formed by the embrittlement effect caused by nitrogen causes an increase in the wear rate in the dry nitrogen environment, and when oil is used, the oil film between the pin and the contact surface causes easy slip at lower shear stresses, resulting in low wear rates (Figs. 7e,f). In the wear tests carried out under vacuum conditions, it was seen that the transfer film was also formed in the DLC-coated samples, but the debris was agglomerated between the pin and the substrate with the effect of vacuum (Fig. 7g). The morphology of wear depths was supported by the three-dimensional (3D) optical profilometry images of both untreated and coated surfaces (Fig. 8). In Fig. 8a, it was observed that the penetration depth of the pin on the untreated sample was deeper than the other samples because it had relatively low surface hardness and accordingly low load-bearing capacity/plastic deformation resistance [35]. After the coatings, more superficial and narrow wear marks were obtained (Figs. 8b,c). The narrowest and most superficial wear track was obtained in DLC-coated samples (Fig. 8d).

4. Conclusions

In this study, the tribological properties of TiN, CrN, and DLC films deposited at equal thickness and surface roughness values on the AISI high-speed steel substrates were compared under humid air, dry nitrogen, and oil sliding conditions. The conclusions derived from the above results and discussions can be

summarized as follows:

– All deposited films increased the surface hardness of the alloy by 3–4 times. The highest hardness value was obtained from TiN-coated samples.

– Compressive residual stresses occurred in all applied coatings. While the highest internal stress was obtained in TiN-coated samples, the lowest internal stress was obtained in CrN-coated samples.

– It was determined that the most important parameters on wear resistance were hardness, residual stress, adhesion, and especially the chemical composition of the films.

– While all applied coatings in this study reduced the friction coefficient of the samples for all sliding conditions, the lowest friction coefficient value was measured from DLC-coated samples tested in oil sliding conditions. The lowest friction coefficient values of DLC coatings were ascribed to the formation of a graphitized transfer layer.

– Although each ceramic-based coating applied to the surface in this study improved the wear resistance of the M2 high-speed steel substrates for all sliding conditions. Better wear performance of ceramic-based coated samples was attributed to higher load-bearing capacity and reduced subsurface deformation.

– Considering the wear environments, the highest coefficients of friction and wear rates were obtained under vacuum conditions due to lack of oxidation for untreated sample. DLC coating was a good candidate considering all tribo-test environments, even vacuum.

Acknowledgement

The authors would like to thank Erzurum Technical University High Technology Research Center (YUTAM) for valuable contributions.

References

[1] G. R. Piazzetta, L. E. Lagoeiro, I. F. R. Figueira, M. A. G. Rabelo, G. Pintaude, Identification of abrasion regimes based on mechanisms of wear on the steel stylus used in the Cerchar abrasiveness test, Wear 410–411 (2018) 181–189. https://doi.org/10.1016/j.wear.2018.07.009

[2] X. L. Wang, K. Adachi, K. Otsuka, K. Kato, Optimization of the surface texture for silicon carbide sliding in water, Appl. Surf. Sci. 253 (2006) 1282–1286. https://doi.org/10.1016/j.apsusc.2006.01.076

[3] H. W. Yu, W. Huang, X. L. Wang, Dimple patterns design for different circumstances, Lubr. Sci. 25 (2013) 67–78. https://doi.org/10.1002/ls.168

[4] W. Zhang, A novel ceramic with low friction and wear toward tribological applications: Boron carbide-silicon carbide, Adv. Colloid Interface Sci. 301 (2022) 102604. https://doi.org/10.1016/j.cis.2022.102604

[5] W. Zhang, Tribology of SiC ceramics under lubrication: Features, developments, and perspectives, Curr. Opin. Solid State Mater. Sci. 26 (2022) 101000. https://doi.org/10.1016/j.cossms.2022.101000

[6] E. E. Vera, M. Vite, R. Lewis, E. A. Gallardo, J. R. Laguna-Camacho, A study of the wear performance of TiN, CrN and WC/C coatings on different steel substrates, Wear 271 (2011) 2116–2124. https://doi.org/10.1016/j.wear.2010.12.061

[7] I. Hacisalihoglu, F. Yildiz, A. Alsaran, Wear performance of different nitride-based coatings on plasma nitrided AISI M2 tool steel in dry and lubricated conditions, Wear 384–385 (2017) 159–168. https://doi.org/10.1016/j.wear.2017.01.117

[8] H. Çalişkan, P. Panjan, S. Paskvale, Monitoring of wear characteristics of TiN and TiAlN coatings at long sliding distances, Tribol. Trans. 57 (2014) 496–502. https://doi.org/10.1080/10402004.2014.884254

[9] S. Kumar, S. R. Maity, L. Patnaik, Effect of tribological process parameters on the wear and frictional behaviour of Cr-(CrN/TiN) composite coating: An experimental and analytical study, Ceram. Int. 47 (2021) 16018–16028. https://doi.org/10.1016/j.ceramint.2021.02.176

[10] H. Kovacı, Y. B. Bozkurt, A. F. Yetim, Ö. Baran, A. Çelik, Corrosion and tribocorrosion properties of duplex surface treatments consisting of plasma nitriding and DLC coating, Tribol. Int. 156 (2021) 106823. https://doi.org/10.1016/j.triboint.2020.106823

[11] H. Kovacı, A. F. Yetim, Ö. Baran, A. Çelik, Tribological behavior of DLC films and duplex ceramic coatings under different sliding conditions, Ceram. Int. 44 (2018) 7151–7158. https://doi.org/10.1016/j.ceramint.2018.01.158

[12] A. Liu, J. Deng, H. Cui, Y. Chen, J. Zhao, Friction and wear properties of TiN, TiAlN, AlTiN and CrAlN PVD nitride coatings, Int. J. Refract. Met. Hard Mater. 31 (2012) 82–88. https://doi.org/10.1016/j.ijrmhm.2011.09.010

[13] I. Efeoglu, Ö. Baran, F. Yetim, S. Altintaş, Tribological characteristics of MoS2-Nb solid lubricant film in different tribo-test conditions, Surf. Coatings Technol. 203 (2008) 766–770. https://doi.org/10.1016/j.surfcoat.2008.08.048

[14] F. Yildiz, A. F. Yetim, A. Alsaran, A. Çelik, Plasma nitriding behavior of Ti6Al4V orthopedic alloy, Surf. Coatings Technol. 202 (2008) 2471–2476. https://doi.org/10.1016/j.surfcoat.2007.08.004

[15] J. W. Du, L. Chen, J. Chen, Y. Du, Mechanical properties, thermal stability and oxidation resistance of TiN/CrN multilayer coatings, Vacuum 179 (2020) 109468. https://doi.org/10.1016/j.vacuum.2020.109468

[16] Z. Zhang, J. Chen, G. He, G. Yang, Fatigue and mechanical behavior of Ti-6Al-4V alloy with CrN and TiN coating deposited by magnetic filtered cathodic vacuum arc process, Coatings 9 (2019) 1–13. https://doi.org/10.3390/coatings9100689

[17] L. Shan, Y. Wang, J. Li, J. Chen, Effect of N_2 flow rate on microstructure and mechanical properties of PVD CrN_x coatings for tribological application in seawater, Surf. Coatings Technol. 242 (2014) 74–82. https://doi.org/10.1016/j.surfcoat.2014.01.021

[18] A. Wilson, A. Matthews, J. Housden, R. Turner, B. Garside, A comparison of the wear and fatigue properties of plasma-assisted physical vapour

deposition TiN, CrN and duplex coatings on Ti-6Al-4V, Surf. Coatings Technol. 62 (1993) 600–607. https://doi.org/10.1016/0257-8972(93)90306-9
[19] H. Schulz, E. Bergmann, Properties and applications of ion-plated coatings in the system CrCN, Surf. Coatings Technol. 50 (1991) 53–56. https://doi.org/10.1016/0257-8972(91)90192-Y
[20] C. Lorenzo-Martin, O. Ajayi, A. Erdemir, G. R. Fenske, R. Wei, Effect of microstructure and thickness on the friction and wear behavior of CrN coatings, Wear 302 (2013) 963–971. https://doi.org/10.1016/j.wear.2013.02.005
[21] Y. G. Yang, R. A. Johnson, H. N. G. Wadley, A Monte Carlo simulation of the physical vapor deposition of nickel, Acta Mater. 45 (1997) 1455–1468. https://doi.org/10.1016/S1359-6454(96)00256-X
[22] S. H. Yao, Y. L. Su, The tribological potential of CrN and Cr(C,N) deposited by multi-arc PVD process, Wear 212 (1997) 85–94. https://doi.org/10.1016/S0043-1648(97)00128-2
[23] N. S. Mansoor, A. Fattah-alhosseini, H. Elmkhah, A. Shishehian, Comparison of the mechanical properties and electrochemical behavior of TiN and CrN single-layer and CrN/TiN multi-layer coatings deposited by PVD method on a dental alloy, Mater. Res. Express 6 (2019) 126433. https://doi.org/10.1088/2053-1591/ab640d
[24] Y. L. Su, S. H. Yao, Z. L. Leu, C. S. Wei, C. T. Wu, Comparison of tribological behavior of three films – TiN, TiCN and CrN– grown by physical vapor deposition, Wear 213 (1997) 165–174. https://doi.org/10.1016/S0043-1648(97)00182-8
[25] H. Kovacı, Ö. Baran, A. F. Yetim, Y. B. Bozkurt, L. Kara, A. Çelik, The friction and wear performance of DLC coatings deposited on plasma nitrided AISI 4140 steel by magnetron sputtering under air and vacuum conditions, Surf. Coatings Technol. 349 (2018) 969–979. https://doi.org/10.1016/j.surfcoat.2018.05.084
[26] A. Erdemir, O. L. Eryilmaz, S. H. Kim, Effect of tribochemistry on lubricity of DLC films in hydrogen, Surf. Coatings Technol. 257 (2014) 241–246. https://doi.org/10.1016/j.surfcoat.2014.08.002
[27] A. Erdemir, C. Donnet, Tribology of diamond-like carbon films: Recent progress and future prospects, J. Phys. D: Appl. Phys. 39 (2006) R311. https://doi.org/10.1088/0022-3727/39/18/R01
[28] J. Robertson, Diamond-like amorphous carbon, Mater. Sci. Eng.: R: Reports 37 (2002) 129–281. https://doi.org/10.1016/S0927-796X(02)00005-0
[29] A. F. Yetim, Investigation of wear behavior of titanium oxide films, produced by anodic oxidation, on commercially pure titanium in vacuum conditions, Surf. Coatings Technol. 205 (2010) 1757–1763. https://doi.org/10.1016/j.surfcoat.2010.08.079
[30] T. Haque, A. Morina, A. Neville, R. Kapadia, S. Arrowsmith, Effect of oil additives on the durability of hydrogenated DLC coating under boundary lubrication conditions, Wear 266 (2009) 147–157. https://doi.org/10.1016/j.wear.2008.06.011
[31] S. Rabadzhiyska, L. Kolaklieva, V. Chitanov, T. Cholakova, R. Kakanakov, N. Dimcheva, K. Balashev, Mechanical, wear and corrosion behavior of CrN/TiN multilayer coatings deposited by low temperature unbalanced magnetron sputtering for biomedical applications, Mater. Today Proc. 5 (2018) 16012–16021. https://doi.org/10.1016/j.matpr.2018.05.046
[32] R. Ramadoss, N. Kumar, S. Dash, D. Arivuoli, A. K. Tyagi, Wear mechanism of CrN/NbN superlattice coating sliding against various counterbodies, Int. J. Refract. Met. Hard Mater. 41 (2013) 547–552. https://doi.org/10.1016/j.ijrmhm.2013.07.005
[33] P. J. Withers, H. K. D. H. Bhadeshia, Residual stress. Part 1 – Measurement techniques, Mater. Sci. Technol. 17 (2001) 355–365. https://doi.org/10.1179/026708301101509980
[34] S. J. Bull, Failure mode maps in the thin film scratch adhesion test, Tribol. Int. 30 (1997) 491–498. https://doi.org/10.1016/S0301-679X(97)00012-1
[35] H. Kovaci, Hacisalihoğlu, A. F. Yetim, A. Çelik, Effects of shot peening pre-treatment and plasma nitriding parameters on the structural, mechanical and tribological properties of AISI 4140 low-alloy steel, Surf. Coatings Technol. 358 (2019) 256–265. https://doi.org/10.1016/j.surfcoat.2018.11.043